Effect of TiO_2 Nanoparticles Addition on the Electrochemical Migration of Lead-Free Sn-Bi Alloys

Ali Dayoub[1)], Ali Gharaibeh[1)], Patrik Tamási[2], Petr Veselý[3)], Markéta Klimtová[3)], Iva Králová[3)], Karel Dušek[3)] and Bálint Medgyes[1)]

[1)]Department of Electronics Technology, Faculty of Electrical Engineering and Informatics, Budapest University of Technology and Economics, Műegyetem rkp. 3., H-1111 Budapest, Hungary

[2)]Continental Automotive Hungary Kft, Napmátka u. 6, H-1106, Budapest, Hungary

[3)]Department of Electrotechnology, Faculty of Electrical Engineering, Czech Technical University in Prague, Prague, Czech Republic

ali.dayoub@edu.bme.hu

***Abstract*—This research aimed to investigate the susceptibility of Sn-58Bi alloys to Electrochemical Migration (ECM) when combined with TiO_2 nanoparticles in various solutions, including deionized water (DI), 1 mM Na_2SO_4, 500 mM Na_2SO_4, 1 mM NaCl, and 500 mM NaCl, using water drop (WD) tests. The results revealed a heightened ECM susceptibility in Sn-58Bi alloys with the addition of TiO_2 nanoparticles, indicating an adverse impact of TiO_2 nanoparticle incorporation. Furthermore, scanning electron microscopy and energy dispersive X-ray spectroscopy (SEM-EDS) were utilized to analyze the surface morphology and elemental composition of dendrites formed after the WD tests. The outcomes showed the presence of dendrites and precipitates in both Sn-58Bi and Sn-58Bi-0.1% TiO_2 cases. Sn was identified as the primary element in the dendrites, while Bi was not detected in the dendrites in any of the cases. Consequently, the reliability of electronics may be compromised when using Bi-Sn paste doped with TiO_2 nanoparticles, particularly in terms of ECM. Nonetheless, these nanoparticles could enhance other properties associated with modified microstructure, such as mechanical or thermal properties, which warrant further investigation.**

Keywords—Reliability of Electronics, ceramic nanoparticles, bismuth-tin alloy, electrochemical migration, dendrite growth

I. INTRODUCTION

Electrochemical migration (ECM), a type of electrochemical corrosion, occurs between two electrodes with opposing biases while submerged in an electrolyte [1]. This corrosion encourages the growth of dendrites from the cathode to the anode, leading to compromised insulation resistance and eventual electronic failure during operation. Studies suggest that the degree of electronic failures due to the ECM differs based on operational parameters [2], [3]. As electronic systems become smaller and the industry shifts away from the lead, comprehending ECM becomes progressively important [2].

Tin-based solder alloys have emerged as promising substitutes for those containing lead. Several factors, such as voltage level [4], [5], spacing [4], and the presence and concentration of impurities [6], [7], have a significant impact on the ECM behavior of these lead-free alloys. Among them, the tin-silver-copper alloy (SAC) receives considerable attention due to its impressive mechanical properties and weldability [8]. However, low-temperature alloys, which melt below 180 °C, are also crucial. Their utilization is essential, especially for tasks involving the fabrication of welding-based 3D structures, except in situations requiring rework operations or with temperature-sensitive components [9].

There is a continual effort to improve the durability of solder joints, to strengthen their ability to withstand mechanical strain and thermal stress, thereby increasing their resistance to ECM. One potential approach is to integrate nanoparticles (NPs) made of metallic elements that differ from those found in the base alloy. However, this approach is limited by the post-consolidation melting temperature of the alloy. In the case of low-temperature brazing alloys, introducing additional common metal elements can raise the melting point, which is undesirable as it undermines the intended enhancement [9].

To overcome this obstacle in various alloys and achieve improved microstructure, a strategy entails uniformly and consistently distributing nanoparticles within the solder paste throughout the material intended for welding. This technique has been utilized to integrate Ag [10], Cu [11], Ni [12], Ti [13], Co [14], and Cr [15]. The effectiveness of this method was evaluated in the context of Bi-Sn alloy.

Weld joints containing Ag and Ti NPs experienced a notable increase in shear strength [10], [13]. In contrast, the addition of Cu and Ni resulted in only marginal improvements in mechanical strength, hardness, and resistance to creep [12], [13]. The introduction of Co effectively reduced the thickness of intermetallic compound (IMC) interfaces and significantly controlled their expansion during thermal aging [14]. Furthermore, increasing the Cr content led to a shift in self-corrosion potential towards less negative values. Particularly, at a Cr concentration of 0.3 wt.%, the corrosion current density was minimized, resulting in the slowest corrosion rate and indicating superior corrosion resistance [15].

Instead of employing metallic NPs, ceramic NPs like TiO_2, ZnO, AlN, Al_2O_3, ZrO_2, SiO_2, SnO_2, and others provide a choice. Studies indicate that integrating TiO_2 NPs into SAC solder, referred to as SAC + TiO_2, can effectively inhibit dendrite formation in SAC305 alloy [24].

The influence of ceramics on Sn-Bi solder pastes has not been extensively investigated, except in a few cases. Rajendran et al. [16] illustrated that ZnO NPs could improve wettability. Similarly, Wang et al. [17] observed enhanced wettability with the inclusion of AlN NPs. Hu et al. [18] found that incorporating Al2O3 NPs reduces the growth of IMCs under electromigration (electro-thermal) conditions. TiO_2 NPs were noted to significantly impact the shear strength and hardness of reinforced solder joints [19]. However, Veselý's examination [9] revealed an opposite outcome when TiO_2 nanoparticles were introduced to Sn42Bi58, resulting in a decrease in the average failure time.

Due to the limited comprehension of the effects associated with integrating TiO_2 NPs into Bi-Sn solder paste, the current work presents the findings of the ECM behavior of Sn-Bi when being doped with 0.1 wt.% TiO_2 NPs at different solution electrolyte at 10 V bias voltages .

II. Materials and Methods

A. The process of preparing composite solder paste

For solder paste preparation, a commercially accessible product was employed, Indium5.7LT-1 (Indium Corporation, USA), supplied in a 500g container. The container's contents were split into two equal portions. The initial portion remained unaltered (referred to as Paste A), while the second portion was blended with 0.1 wt.% of TiO_2 powder obtained from Sigma Aldrich, USA (referred to as Paste B). A comprehensive mixing was achieved by subjecting the materials to a 15-minute mixing process using the YX500S mixer machine.

The soldering alloy utilized was 58Bi42Sn, comprising particles ranging in size from 25 to 45 μm, with a flux content of 10 wt.%. The TiO_2 powder utilized was of the rutile anatase type, with particle sizes below 100 nm, a molecular weight of 79.87 g/mol, and a trace metal basis of 99.5%.

B. Preparation of test samples

Fig. 1 illustrates the configuration of the test specimens. Each specimen consisted of seven patterns specifically designed for ECM testing, following the guidelines specified in the international standard IPC-TM-650 2.6.3.3. The traces were 0.4 mm wide, with a 0.5 mm gap between electrodes. Two types of test boards were employed: one featuring copper traces without any surface protection (referred to as Cu), and the other with copper traces coated with galvanic gold (galvanic nickel-galvanic gold; referred to as Au). This choice of surface finish aimed to represent commonly utilized options in the electronics industry. Notably, none of the test boards were coated with a solder mask.

The application of solder paste to the test patterns was accomplished using a manual stencil printer SD240 (Spidé, Netherlands) and a laser-cut stencil with a thickness of 150 μm, ensuring an alignment error of no more than 0.1 mm. Following this, the boards underwent reflow in a continuous convection oven Mistral 260 (Spidé, Netherlands).

After reflow, a comprehensive cleaning of all boards was conducted to eliminate solder flux residues. This process entailed utilizing isopropyl alcohol in conjunction with manual cleaning using a soft brush, followed by cleaning in an ultrasonic cleaner with distilled water at 50 °C for 20 minutes, and concluding with drying at 50 °C for three hours. This meticulous procedure guaranteed the absence of visible flux residues between the electrodes.

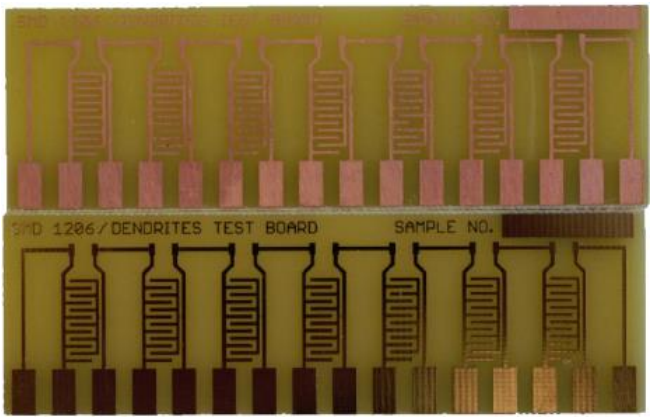

Fig. 1. The utilized the test boards, which include those featuring copper and copper protected by galvanic gold [9].

C. Measurement Methodology

The impact of alloys on ECM was examined alongside TiO_2 NPs across various solutions, including deionized water (DI), 1 mM Na_2SO_4, 500 mM Na_2SO_4, 1 mM NaCl, and 500 mM NaCl, through WD tests. During these tests, a precise pipette dispensed a 10 μl water droplet onto the test pattern, followed by the application of a 10 V bias voltage. To ensure experimental consistency, 14 measurements were carried out for each combination of sample type and solder paste. To characterize the ECM behavior of the tested samples, the time-to-failure (TTF) findings of the WD test were fitted to the 2-P Weibull distribution.

The experimental configuration of the WD test (Fig. 2) includes a laboratory voltage source, a Novus USB data logger, and a USB microscope.

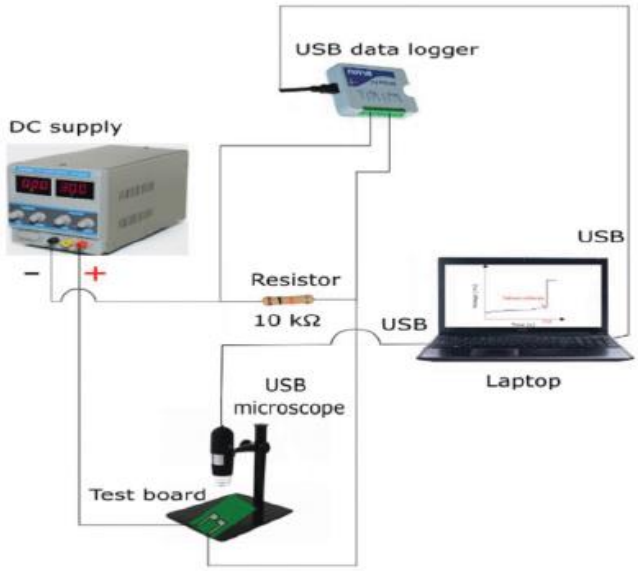

Fig. 2. illustrates the schematic diagram of the water drop test measurement [20].

Moreover, a scanning electron microscope (SEM, FEI Inspect S50) with energy dispersive spectroscopy (EDX) capabilities (Bruker Quanta EDX) were performed to observe the dendrite structure and ascertain the elemental composition.

III. Results

A. Results of WD test

The TTF results obtained from the WD tests are depicted in Figs. 3-5. The data revealed a noticeable decline in Mean Time to Failure (MTTF) upon the inclusion of TiO_2 NPs in the solder. Short circuits were observed to manifest sooner for Paste B compared to the unmodified solder paste (A).

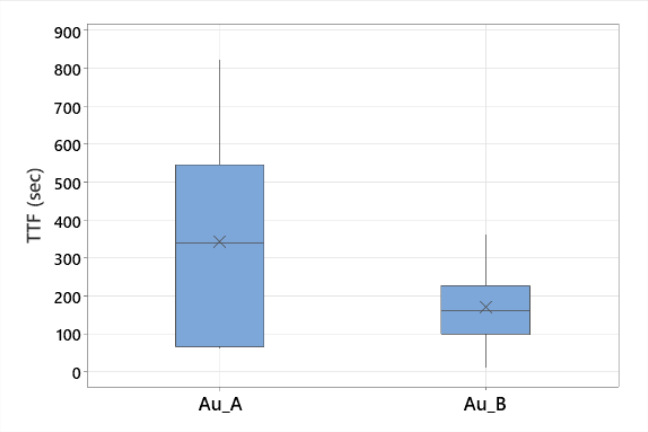

Fig. 3. TTF data upon the Addition of TiO_2 NPs in DI water at 10 VDC bias voltage– (x represents the MTTF).

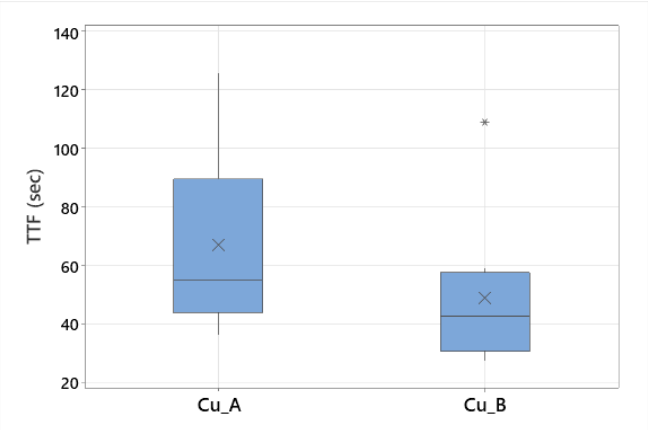

Fig. 4. TTF data upon the Addition of TiO_2 NPs in 500 mM Nacl at 10 VDC bias voltage– (x represents the MTTF).

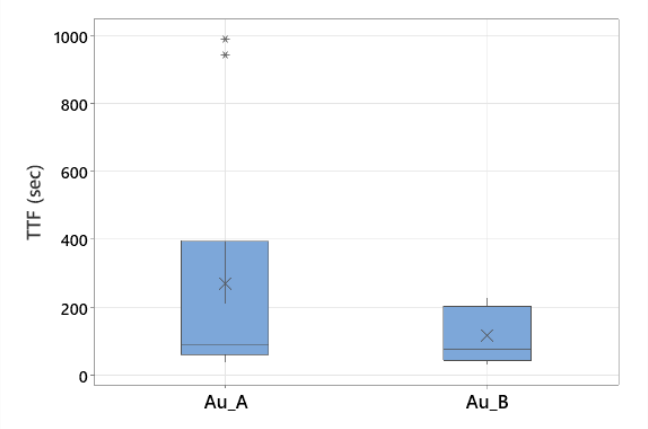

Fig. 5. TTF data upon the Addition of TiO_2 NPs in 500 mM Na_2SO_4 at 10 VDC bias voltage– (x represents the MTTF).

Table 1 displays the parameters of the Weibull distribution, including the shape parameter (β) and the scale parameter (η). β indicates the rate at which the failure rate changes over time, while η represents the characteristic life or scale of the distribution. Specifically, η denotes the point in time when approximately 63.2% of the population will have experienced failure.

TABLE I. WEIBULL PARAMETERS FOR THE EXAMINED SOLDERS

Solders	**Weibull Parameters**	
	β	***η (sec)***
Au_A – DI	1.31	370.40
Au_B – DI	1.48	183.72
Cu_A - 500 mM NaCl	2.42	75.82
Cu_B - 500 mM NaCl	2.22	55.12
Au_A - 500 mM Na_2SO_4	0.83	239.26
Au_B - 500 mM Na_2SO_4	1.48	127.71

Furthermore, Fig. 6 presents data on the MTTF of Au_A under various types of contaminants. It was observed that the failure time was immediate when exposed to a 1 mM NaCl solution, whereas its duration was shorter in a 1 mM Na_2SO_4 solution compared to deionized water. It is important to highlight that ionic contaminants expedite the ECM process. This acceleration occurs as the electrolyte's conductivity rises with the increasing number of dissociated ionic species in the solution. Consequently, this heightened conductivity enhances the "aggressiveness" of the electrolytes, leading to a swifter anodic dissolution [21], [22].

The effect of ionic contaminants becomes apparent when considering a 1 mM NaCl solution, where ECM failure occurs almost instantaneously. Furthermore, Fig. 6 additionally indicates that the NaCl solution exhibits greater aggressiveness compared to the Na_2SO_4 solution. Unfortunately, chloride ions (Cl^-) stand out as the predominant corrosive contaminant in various environmental settings. They can originate from diverse sources such as human sweat, fingerprints, airborne dust, residues from manufacturing processes, degradation of packaging materials, and even salt spray from marine environments [23].

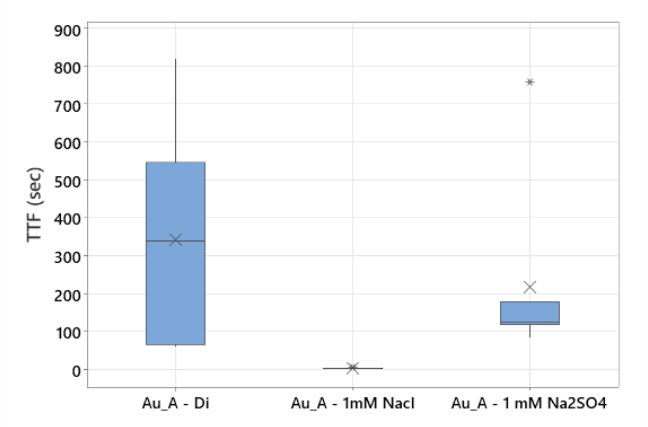

Fig. 6. TTF data of Au_A under various types of contaminants at 10 VDC bias voltage– (x represents the MTTF).

B. Results of SEM-EDS methods

SEM-EDS analysis was carried out to investigate the surface morphology and elemental composition of dendrites and residues post-WD testing.

In the presence of 1mM Na_2SO_4, Au_A showcased a combination of trunk and lace-like structures, as illustrated in Fig. 7, while Au_B exhibited a lace-like morphology under identical conditions, as depicted in Fig. 8. This difference in the morphology of the dendrites might be attributed to the impact of nanoparticle incorporation on the solder paste.

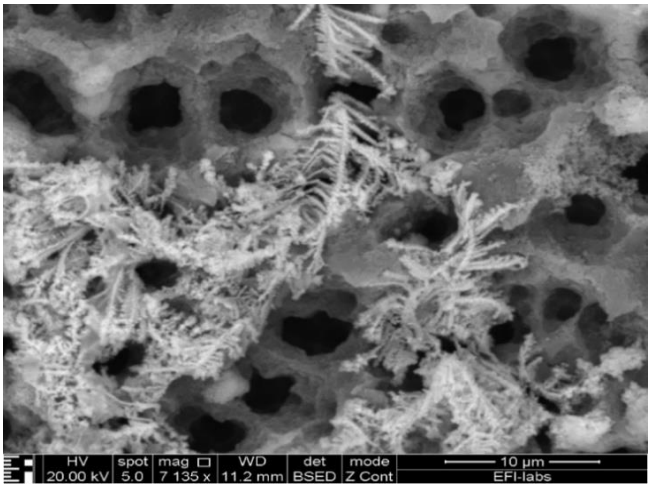

Fig. 7. Dendrites from Au_A after WD test in 1mM Na_2SO_4 solution at 10 VDC.

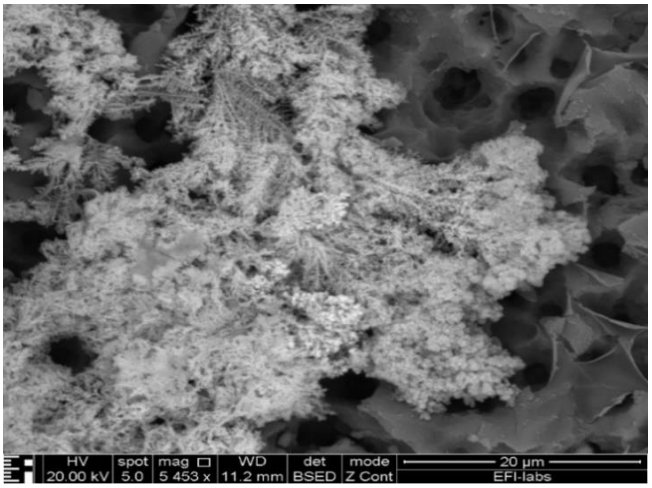

Fig. 8. Dendrites from Au_B after WD test in 1mM Na_2SO_4 solution at 10 VDC.

Considering the influence of changing the type of contaminants on Au_B with 500 mM Na_2SO_4, the morphology of the dendrites revealed a blend of fishbone-like structures, straight, and perpendicular branching forms, as shown in Fig. 9. Conversely, the dendrites formed in the case of Cu_A exposed to 500 mM NaCl exhibited a fishbone-like structure, as depicted in Fig. 10.

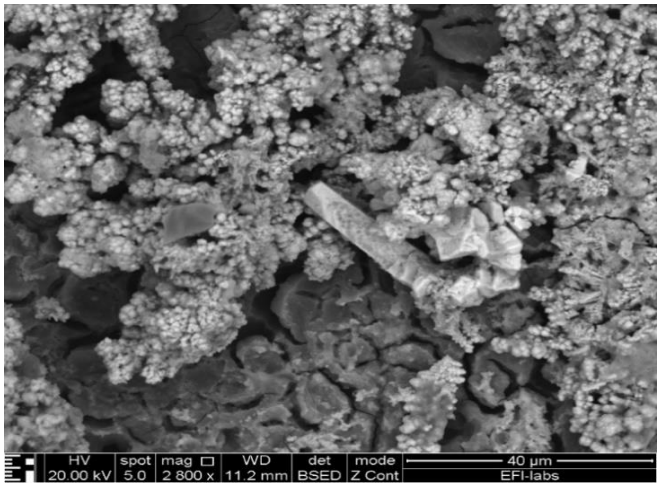

Fig. 9. Dendrites from Au_B after WD test in 500 mM Na_2SO_4 solution at 10 VDC.

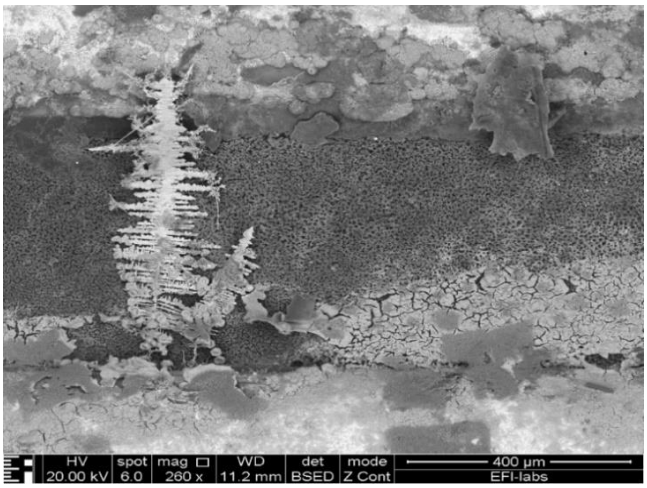

Fig. 10. Dendrites from Cu_A after WD test in 500 mM NaCl solution at 10 VDC.

While prior research presents conflicting views on the impact of incorporating TiO_2 NPs into solder alloys, certain studies have suggested a beneficial outcome by inhibiting dendrite growth when introduced to SAC305 alloy [24]. Nevertheless, the study in [25] did not observe substantial suppression or alteration in dendrite morphology, while other investigations reported adverse effects upon adding TiO_2 NPs to 58Bi42Sn [9]. Hence, the extent to which the addition influences ECM behavior of lead-free solder alloy remains unresolved in previous literature.

In our study, concerning the Sn-Bi alloy utilized, dendritic formations on Au samples generally exhibited greater branching compared to those on Cu samples. In addition to dendrites, surface precipitates, likely comprising Sn(OH)2, were observed. It is theorized that alterations in dendrite morphology could substantially influence ECM properties. Dendrites characterized by straight and perpendicular branching morphology may experience shorter propagation times than those displaying a combination of trunk and lace-type morphology [26]. Table 2 outlines the outcomes derived from EDS analysis of dendrites resulting from ECM WD tests. It is evident that Sn consistently emerges as the predominant element within the dendrites across all scenarios. Following Sn, Cu is detected, likely due to its inclusion in the base material utilized for sample fabrication. Notably, Au was not detected; instead, Br, Ni, and S might be have originated from the FR4 substrate, along with precipitates formed during the WD test. Noteworthy is the minor presence of Na and Cl in the dendrites, attributed to electrolyte residues from the WD test. However, Bi was absent from the dendrites, suggesting its non-involvement in the migration process, contrary to previous assertions [9].

TABLE II. EDS RESULTS FROM THE DENDRITES OF SN-BI-(0.1, 1% TIO_2)

Solders	**Dendrites Composition (wt.%)**						
	Na	***S***	***Cl***	***Ni***	***Cu***	***Br***	***Sn***
Cu_A_0.5 M NaCl	0.3	-	0.8	-	-	3.1	95.8
Au_B_0.5 M Na_2SO_4	2.1	1.6	-	-	18.6	-	77.7
Au_A_1m M Na_2SO_4	-	-	-	8	9.5	11.1	71.4
Au_B_1m M Na_2SO_4	-	-	-	0.1	5.5	-	94.4

.

I. DISCUSSION

Previous research has highlighted variations in how the inclusion of TiO_2 NPs impacts dendrite formation, contingent upon the alloy type. Specifically, TiO_2 nanoparticles were observed to hinder dendrite formation in SAC alloys, resulting in a prolonged MTTF compared to unmodified solder alloys [24], [25]. Conversely, the MTTF either remained unchanged or decreased for modified solder pastes compared to unmodified ones in Sn-Bi alloy, as reported by [9]. Therefore, further investigation is necessary to attain a comprehensive understanding of the role of TiO_2 NPs in Bi-Sn solders and their influence on solder joint properties. Our study unveiled a reduced MTTF for modified alloys compared to unmodified ones.

Moreover, the increased occurrence of Cu in the dendrites observed in Au_A and Au_B indicates challenges in adequately wetting the copper surface. In areas where copper remains unwetted or exposed, it can readily engage in the ECM process due to its propensity to migrate [27].

The lack of Bi presence in the dendrites was extensively recorded in references [28], [29], [30], [31], [32]. Consequently, it is widely accepted that Bi does not contribute to the formation of dendrites.

II. CONCLUSIONS

The main objective was to improve the performance of the solder alloy concerning ECM, based on insights from prior research. However, contrary to expectations, the outcomes of WD tests unveiled that the modified solder paste displayed heightened susceptibility to ECM compared to the unmodified solder paste. This represents a significant setback in advancing the composite Bi-Sn/TiO_2 NPs concerning ECM considerations. Nevertheless, it is confirmed that Bi remains inert and does not participate in the ECM process, while the ceramic NPs may offer enhancements in other aspects of the solder alloy, such as mechanical or thermal properties. Consequently, further investigation is essential to gain a more comprehensive understanding of the influence of TiO_2 NPs in Bi-Sn solders.

ACKNOWLEDGMENT

The study described in this paper, conducted at BME, has received support from the National Research, Development, and Innovation (NRDI) Office Fund under project FK 138220.

REFERENCES

[1] G. T. KOHMAN, H. W. HERMANCE, and G. H. DOWNES, "Silver Migration in Electrical Insulation," *Bell Syst. Tech. J.*, vol. 34, no. 6, pp. 1115–1147, Nov. 1955.

[2] X. Zhong, L. Chen, B. Medgyes, Z. Zhang, S. Gao, and L. Jakab, "Electrochemical migration of Sn and Sn solder alloys: A review," *RSC Adv.*, vol. 7, no. 45, pp. 28186–28206, May 2017,

[3] N. C. Lee, "Future lead-free solder alloys and fluxes - Meeting challenges of miniaturization," *IPC - IPC Print. Circuits Expo, APEX Des. Summit 2008*, vol. 2, pp. 864–872, 2008.

[4] X. Qi *et al.*, "Electrochemical migration behavior of Sn-based lead-free solder," *J. Mater. Sci. Mater. Electron.*, vol. 30, no. 15, pp. 14695–14702, Jul. 2019,

[5] B. Liao, W. Jia, R. Sun, Z. Chen, and X. Guo, "ELECTROCHEMICAL MIGRATION BEHAVIOR of Sn-3.0Ag-0.5Cu SOLDER ALLOY under THIN ELECTROLYTE LAYERS," *Surf. Rev. Lett.*, vol. 26, no. 6, pp. 1–7, Jun. 2019,

[6] P. Yi, C. Dong, Y. Ji, Y. Yin, J. Yao, and K. Xiao, "Electrochemical migration failure mechanism and dendrite composition characteristics of Sn96.5Ag3.0Cu0.5 alloy in thin electrolyte films," *J. Mater. Sci. Mater. Electron.*, vol. 30, no. 7, pp. 6575–6582, Feb. 2019,

[7] B. Medgyes, E. Román, Á. Bohnert, S. Szurdán, X. Zhong, and G. Harsányi, "Electrochemical Migration Investigations on SAC-Bi-xMn Solder Alloys," in *2018 IEEE 24th International Symposium for Design and Technology in Electronic Packaging, SIITME 2018 - Proceedings*, Oct. 2018, pp. 80–83.

[8] L. Hua, H. N. Hou, H. Q. Zhang, T. Wu, and Y. H. Deng, "Effects of Zn, Ge doping on electrochemical migration, oxidation characteristics and corrosion behavior of lead-free Sn-3.0Ag-0.5Cu solder for electronic packaging," in *Proceedings - 2010 11th International Conference on Electronic Packaging Technology and High Density Packaging, ICEPT-HDP 2010*, 2010, pp. 1151–1157.

[9] P. Veselý, D. Froš, M. Klimtová, A. Gharaibeh, and B. Medgyes, "Effect of Incorporation of Ceramic Nanoparticles in Bismuth-Tin Solder Paste on Electrochemical Migration," in *2023 46th International Spring Seminar on Electronics Technology (ISSE)*, Timisoara, Romania, 2023, pp. 1–6.

[10] I. Shafiq and Y. C. Chan, "Improved electro-migration resistance in nano Ag modified Sn-58Bi solder joints under current stressing," Xi'an, China, 2011.

[11] N. Jiang *et al.*, "Influences of doping Ti nanoparticles on microstructure and properties of Sn58Bi solder," *J. Mater. Sci. Mater. Electron.*, vol. 30, no. 19, pp. 17583–17590, Aug. 2019,

[12] Y. Liu, H. Zhang, and F. Sun, "Solderability of SnBi-nano Cu solder pastes and microstructure of the solder joints," *J. Mater. Sci. Mater. Electron.*, vol. 27, no. 3, pp. 2235–2241, Nov. 2016,

[13] L. Shen, Z. Y. Tan, and Z. Chen, "Nanoindentation study on the creep resistance of SnBi solder alloy with reactive nano-metallic fillers," *Mater. Sci. Eng. A*, vol. 561, pp. 232–238, 2013,

[14] M. Nasir Bashir *et al.*, "Effect of cobalt nanoparticles on mechanical properties of Sn–58Bi solder joint," *J. Mater. Sci. Mater. Electron.*, vol. 33, no. 28, pp. 22573–22579, Aug. 2022,

[15] Q. Song, A. Li, D. Qi, W. Qin, Y. Li, and Y. Zhan, "The electrochemical corrosion behavior of Sn58Bi-XCr composite solder," *Mater. Chem. Phys.*, vol. 295, no. March 2022, pp. 0254–0584, Nov. 2023,

[16] S. H. Rajendran, H. Kang, and J. P. Jung, "Ultrasonic-Assisted Dispersion of ZnO Nanoparticles to Sn-Bi Solder: A Study on Microstructure, Spreading, and Mechanical Properties," *J. Mater. Eng. Perform.*, vol. 30, no. 5, pp. 3167–3172, 2021,

[17] X. Wang, L. Zhang, M. lan Li, X. Wang, and M. Zhao, "Enhancement of structure and properties of Sn58Bi solder by AlN ceramic particles," *J. Mater. Res. Technol.*, vol. 19, pp. 2584–2595, Jun. 2022,

[18] T. Hu, Y. Li, Y. C. Chan, and F. Wu, "Effect of nano Al2O3 particles doping on electromigration and mechanical properties of Sn-58Bi solder joints," *Microelectron. Reliab.*, vol. 55, no. 8, pp. 1226–1233, May 2015,

[19] S. Amares and B. Tchari, "Effect on Shear Strength and Hardness Properties of Tin Based Solder Alloy, Sn-50Bi, Sn-50Bi+2%TiO2 Nanoparticles," *Adv. Mater. Res.*, vol. 1159, pp. 54–59, May 2020,

[20] A. Gharaibeh, D. Rigler, B. Medgyes, and G. Harsanyi, "Electrochemical Migration Investigation on Lead-Free Sn-based Solder Alloys in 3.5 wt.% NaCl Solution," in *Proceedings of the International Spring Seminar on Electronics Technology*, Vienna, Austria, 2022, pp. 5–9.

[21] X. Zhong, G. Zhang, Y. Qiu, Z. Chen, and X. Guo, "Electrochemical migration of tin in thin electrolyte layer containing chloride ions," *Corros. Sci.*, vol. 74, pp. 71–82, Apr. 2013,

[22] Y. Zhou, Y. Li, Y. Zhao, and W. Lu, "Electrochemical Migration of Immersion Silver Plated Printed Circuit Boards Contaminated by Dust Solution," *IEEE Trans. Device Mater. Reliab.*, vol. 21, no. 1, pp. 117–128, Mar. 2021,

[23] G. Harsányi, "Irregular effect of chloride impurities on migration failure reliability: Contradictions or understandable?," *Microelectron. Reliab.*, vol. 39, no. 9, pp. 1407–1411, 1999,

[24] N. K. Othman, F. R. Omar, and F. Che Ani, "Electrochemical migration and corrosion behaviours of SAC305 reinforced by NiO, Fe2O3, TiO2 nanoparticles in NaCl solution," in *IOP Conference Series: Materials Science and Engineering*, 2019.

[25] A. Gharaibeh and B. Medgyes, "Electrochemical migration investigation on SAC alloys incorporated by TiO2nanoparticles in NaCl solution," in *2022 IEEE 9th Electronics System-Integration Technology Conference, ESTC 2022 - Proceedings*, Sibiu, Romania, 2022, pp. 484–487.

[26] A. Gharaibeh, D. Rigler, and B. Medgyes, "Effect of TiO2 Nanoparticles Addition on the Electrochemical Migration of Low-Silver Lead-Free SAC Alloys," in *2023 46th International Spring Seminar on Electronics Technology (ISSE)*, Timisoara, Romania, 2023, pp. 1–5.

[27] B. Medgyes, B. Illés, and G. Harsányi, "Electrochemical migration behaviour of Cu, Sn, Ag and Sn63/Pb37," *J. Mater. Sci. Mater. Electron.*, vol. 23, no. 2, pp. 551–556, Jun. 2012,

[28] L. Hua and H. Hou, “Electrochemical migration behaviors of lead-free 64Sn-35Bi-1Ag solder on FR-4 PCB board plated with Cu,” *Wuhan Univ. J. Nat. Sci.*, vol. 17, no. 1, pp. 79–85, 2012,

[29] L. Hua and H. N. Hou, “Electrochemical corrosion and electrochemical migration of 64Sn-35Bi-1Ag solder doping with xGe on printed circuit boards,” *Microelectron. Reliab.*, vol. 75, pp. 27–36, 2017,

[30] Y. R. Yoo and Y. S. Kim, “Influence of electrochemical properties on electrochemical migration of SnPb and SnBi solders,” *Met. Mater. Int.*, vol. 16, no. 5, pp. 739–745, 2010,

[31] D. Q. Yu, W. Jillek, and E. Schmitt, “Electrochemical migration of lead free solder joints,” *J. Mater. Sci. Mater. Electron.*, vol. 17, no. 3, pp. 229–241, 2006,

[32] D. Q. Yu, W. Jillek, and E. Schmitt, “Electrochemical migration of Sn-Pb and lead free solder alloys under distilled water,” *J. Mater. Sci. Mater. Electron.*, vol. 17, no. 3, pp. 219–227, 2006,